

## Treatment of Inflammatory and Neuropathic Pain by Uncoupling Src from the NMDA Receptor Complex

Xue Jun Liu<sup>1,2,3</sup>, Jeffrey R. Gingrich<sup>1,2</sup>, Mariana Vargas-Caballero<sup>1,2</sup>, Yi Na Dong<sup>1,2,3</sup>, Ameet Sengar<sup>1,2</sup>, Simon Beggs<sup>1,2,3</sup>, Szu-Han Wang<sup>1,2</sup>, Hoi Ki Ding<sup>1,2</sup>, Paul W. Frankland<sup>1,2</sup>, and Michael W. Salter<sup>1,2,3</sup>

<sup>1</sup>Program in Neurosciences & Mental Health, the Hospital for Sick Children, Toronto, Ontario, M5G 1X8, Canada

<sup>2</sup>Department of Physiology, Toronto, Ontario, M5G 1X8, Canada

<sup>3</sup>University of Toronto Centre for the Study of Pain, Toronto, Ontario, M5G 1X8, Canada

### Abstract

Chronic pain hypersensitivity depends upon N-methyl-D-aspartate receptors (NMDARs). However, clinical use of NMDAR blockers is limited by side effects from suppressing physiological functions of these receptors. Here we report a means to suppress pain hypersensitivity without blocking NMDARs but rather by inhibiting the binding of a key enhancer of NMDAR function, the protein tyrosine kinase Src. We show that a peptide consisting of amino acids 40–49 of Src fused to the protein transduction domain of the HIV Tat protein (Src40–49Tat) prevented pain behaviors induced by intraplantar formalin and reversed pain hypersensitivity produced by intraplantar injection of complete Freund's adjuvant or by peripheral nerve injury. Src40–49Tat had no effect on basal sensory thresholds, acute nociceptive responses, or cardiovascular, respiratory, locomotor or cognitive functions. Thus, by targeting Src-mediated enhancement of NMDARs, inflammatory and neuropathic pain are suppressed without deleterious consequences of directly blocking NMDARs, an approach that may be of broad relevance to managing chronic pain.

---

Chronic pain is categorized as inflammatory or neuropathic, each involving neuroplastic changes leading to hypersensitivity in peripheral and central nociceptive systems<sup>1,2</sup>. Multiple mechanisms including increased primary afferent excitability<sup>3</sup>, enhanced transmission in the dorsal horn<sup>1</sup>, changes in gene expression<sup>4</sup>, aberrant neuron-glia interactions<sup>5,6</sup> and neuronal apoptosis<sup>7</sup> are implicated in hypersensitivity in chronic pain models. Abundant pre-clinical evidence indicates that N-methyl-D-aspartate receptor (NMDARs)<sup>8</sup> are critically involved in pain hypersensitivity<sup>9–11</sup>. However, pharmacological blockade of these receptors in humans is deleterious because the activity of NMDARs is essential for many important physiological functions including breathing and locomotion<sup>9,12,13</sup>. A crucial signaling event for NMDAR-dependent neuroplasticity, including pain hypersensitivity<sup>1,14</sup>, is upregulation of NMDAR currents by mechanisms including relieving Mg<sup>2+</sup> blockade and receptor phosphorylation<sup>15,16</sup>. Thus, preferentially inhibiting mechanisms which upregulate NMDARs without affecting basal channel activity represents a strategy that may suppress pain hypersensitivity without impairing key physiological functions.

NMDARs are multiprotein complexes comprised of a core tetrameric assembly -- two NR1 subunits and two NR2A-2D subunits – which form the ion channel conductance pathway<sup>8,17</sup>. Within the NMDAR complex, the non-receptor tyrosine kinase Src is a critical regulatory hub through which multiple intracellular signaling cascades converge to increase NMDAR activity<sup>16</sup>. Src is anchored within the NMDAR complex through an adaptor protein which we have identified as NADH dehydrogenase subunit 2 (ND2)<sup>18</sup>. Blocking the interaction between the Src unique domain and ND2 releases Src from the NMDAR complex, separating the enzyme and substrate, thereby inhibiting Src-mediated upregulation of NMDAR activity<sup>18</sup>. Hence, disrupting the Src-ND2 interaction is a strategy to treat pain that not only avoids the undesirable effects of blocking NMDAR function but avoids directly inhibiting the catalytic activity of Src, a widely expressed kinase<sup>19</sup>. In the present study, we tested the hypothesis that uncoupling Src from the NMDAR complex may suppress pain hypersensitivity (Fig. 1a).

## RESULTS

### Constructing a Src-NMDAR uncoupling peptide for use *in vivo*

In order to develop a practical reagent to disrupt anchoring of Src in the NMDAR complex *in vivo*, we synthesized a series of overlapping 10-amino acid peptides covering Src40-58, the region in the unique domain we had previously identified *in vitro* as crucial for the Src-ND2 interaction<sup>18</sup>. We found that a peptide consisting of amino acids 40-49 of Src, Src40-49, but not Src45-54 or Src49-58, bound to ND2.1, the interacting region of ND2 (Fig. 1b). Moreover, Src40-49 disrupted the interaction between the Src unique domain and ND2.1 *in vitro* (Supplementary Fig. 1a).

Intracellular administration of Src40-49 reduced the NMDAR component of the miniature excitatory post-synaptic currents<sup>20</sup> in cultured dorsal horn neurons (Fig. 1c), neurons in which NMDARs are tonically upregulated by Src<sup>14,21,22</sup>. By contrast, administering a peptide with identical amino acid composition but with a scrambled sequence (sSrc40-49) had no effect on synaptic NMDAR currents. The AMPAR component of the mEPSCs was unaffected by either Src40-49 or sSrc40-49. Thus, *in vitro*, Src40-49 disrupts the Src-ND2 interaction and reduces the upregulation of synaptic NMDARs.

Because Src40-49 is predicted to be membrane impermeant, this peptide itself is unsuitable for use *in vivo*. Therefore, we synthesized Src40-49, as well as sSrc40-49, fused to the protein transduction domain of the HIV-1 Tat protein<sup>23</sup>, generating Src40-49Tat and sSrc40-49Tat, respectively. Src40-49Tat, but not sSrc40-49Tat, bound to the ND2.1 fragment of ND2 *in vitro* (Fig 1d). As we had previously observed with Src40-58<sup>18</sup>, Src40-49Tat did not bind to the ND2.2 or ND2.3 fragments of ND2 (Supplementary Fig. 1b). Therefore, adding the Tat protein transduction domain did not abrogate the binding to ND2, and Src40-49Tat retains specificity for the ND2.1 region.

We found next that Src40-49Tat, but not sSrc40-49Tat, disrupted the direct interaction between the Src unique domain and ND2.1 (Fig 1e). Furthermore, by immunoprecipitating either NMDAR complexes or Src from rat brain crude synaptosomes we found that incubating *in vitro* with Src40-49Tat, but not sSrc40-49Tat, suppressed their association

(Fig. 1f,g). Src40-49Tat also suppressed the association of Src with ND2 (Fig. 1g) but had no effect on the interaction between ND2 and NMDARs (Supplementary Fig. 1c), indicating that Src40-49Tat caused a loss of Src from the NMDAR complex by inhibiting the binding of this kinase to ND2. In contrast, Src40-49Tat did not affect the association of Fyn or PSD-95 with NMDARs (Supplementary Fig. 1d,e) demonstrating that this peptide did not generally disrupt interactions between proteins in the NMDAR complex. Moreover, Src40-49Tat had no effect on Src catalytic activity at the concentration which disrupted the Src-ND2 interaction or at 10 times this concentration (Supplementary Fig. 1g), indicating that Src40-49Tat is not a Src kinase inhibitor *per se*.

Administering Src40-49Tat intravenously had no effect on the amount of Src, ND2 or NMDARs in rat brain synaptosomes. However, co-immunoprecipitation of ND2 and of NMDARs with Src was reduced in synaptosomes from animals in which Src40-49Tat had been administered *in vivo* as compared with that in synaptosomes from control rats (Fig. 1h). From the findings collectively, we concluded that Src40-49Tat is suitable for *in vivo* studies on the role of the Src-ND2 interaction in pain hypersensitivity.

### Src40-49Tat prevents formalin-induced pain behaviors

We first tested Src40-49Tat in an inflammatory pain model in which dilute formalin was injected into the rat hindpaw, causing a stereotypic two-phase pattern of behavioral responses<sup>24,25</sup>: phase 1 is independent of NMDARs whereas phase 2 is NMDAR-dependent<sup>4,26</sup>. We found that pretreating with Src40-49Tat (*i.v.* 45 min before formalin), but not sSrc40-49Tat, saline vehicle or Tat-protein transduction domain alone, significantly reduced formalin-induced phase 2 flinching (Fig. 2a,b) and biting or licking behaviors (Supplementary Fig. 2a). In contrast, responses in phase 1 were indistinguishable among all groups tested (Fig. 2c). Moreover, intravenous administration of Src40-49Tat had no effect on formalin-induced paw edema<sup>27</sup> (Fig. 2d).

We then tested Src40-49Tat at 100 times the lowest maximally effective dose, on basal sensory thresholds and locomotor function in naïve rats, and found no alteration in thermal or mechanical thresholds, or rota-rod performance (Supplementary Fig. 2b–d). Src40-49Tat *i.v.* also had no effect on heart rate, respiratory rate or oxygen saturation (Supplementary Table 1). Therefore, administering Src40-49Tat differentially suppresses the second, but not the first, phase of formalin-induced behaviors without causing observable changes in peripheral inflammation, basal sensory thresholds, locomotor performance or cardio-respiratory functions.

In order to determine whether Src40-49Tat may act within the spinal cord to suppress formalin-induced behaviors, we administered the peptide intrathecally at the lumbar level. We found that administering Src40-49Tat *i.t.* 30 min prior to formalin had no effect on behaviors in phase 1 whereas the peptide significantly reduced phase 2 behaviors (Fig. 2e,f, Supplementary Fig. 2e). As the dose of Src40-49Tat *i.t.* was 20 times less than the minimal dose that produced an effect by *i.v.* injection, we concluded that when Src40-49Tat was given intrathecally, the suppression of phase 2 behaviors was mediated within the spinal cord.

We examined the effect of Src40-49Tat on the interactions between Src, ND2 and NMDARs in animals treated with formalin. Intravenously administering Src40-49Tat, but not sSrc40-49Tat, disrupted the association between Src and ND2, and Src and NMDARs in the spinal cord (Fig. 3a), without changing the association between ND2 and NMDARs (Supplementary Fig. 1f). Furthermore, we found that injection of formalin produced an approximately 2.5-fold increase in the level of tyrosine phosphorylation of NR2B subunit of the NMDAR in the lumbar dorsal horn ipsilateral to the formalin injection (Fig. 3b). This increase was prevented by Src40-49Tat (*i.t.*) but not by sSrc40-49Tat (Fig. 3c). Thus, pre-treating with Src40-49Tat suppressed formalin-induced behaviors, disrupted the Src-ND2 interaction in the spinal cord, and reduced the formalin-induced increase in tyrosine phosphorylation of NR2B within the spinal cord.

### Src40-49Tat reverses CFA-induced pain behaviors

We next investigated the effect of Src40-49Tat on established inflammatory pain using thermal and mechanical hypersensitivity evoked by intraplantar injection of Complete Freund's Adjuvant<sup>28</sup> (CFA; Fig. 4). Intravenous administration of Src40-49Tat, but not vehicle or sSrc40-49Tat, caused an increase in the CFA-sensitized paw-withdrawal latency (Fig. 4a,b,c) indicating that the peptide inhibited the established thermal hypersensitivity. The magnitude of reversal of hypersensitivity increased with dose in the range of 0–10 pmol g<sup>-1</sup> and persisted up to 120 min at the maximum dose of Src40-49Tat. Src40-49Tat, but not sSrc40-49Tat, also reversed the increase in tyrosine phosphorylation of NR2B in the ipsilateral spinal dorsal horn that occurred one day after CFA (Fig. 4 inset). Thermal hypersensitivity induced by CFA was also suppressed by intravenous administration of 4-amino-5-(4-chlorophenyl)-7-(*t*-butyl)pyrazolo[3,4-*d*]pyrimidine (PP2), a broad-spectrum inhibitor of Src-family kinases<sup>16</sup>, which had a maximum effect similar to that of Src40-49Tat (Supplementary Fig. 3a,b). The effects of PP2 and Src40-49Tat were not additive, however (Supplementary Fig. 3b), implying that inhibiting Src-kinases broadly produced no further reversal of the CFA-induced thermal hypersensitivity than did Src40-49Tat alone.

Another consequence of intraplantar CFA is mechanical hypersensitivity. We found that mechanical hypersensitivity was suppressed for up to 2 h by Src40-49Tat *i.v.* (Fig. 4d) but unaffected by sSrc40-49Tat. Thus, Src40-49Tat reversed the established thermal and mechanical pain hypersensitivity produced by the inflammatory stimulus CFA.

### Src40-49Tat does not affect learning

We investigated the possible effect of Src40-49Tat on two forms of NMDAR-dependent learning and memory: contextual fear conditioning<sup>29</sup> and conditioned taste aversion<sup>30,31</sup>. In both tasks, we administered Src40-49Tat prior to training and then examined memory 3 days later. For contextual fear conditioning, Src40-49Tat, given intravenously at doses equal or up to 100 times those eliciting maximal suppression of formalin-induced behaviors, produced no change in freezing behavior as compared with saline controls (Supplementary Fig. 4a,b). For conditioned taste aversion, Src 40-49Tat was microinfused bilaterally into the insular cortex 30 min prior to training. Src40-49Tat had no effect on taste preference during the choice test (supplementary Fig. 4d). As a positive control for the injection site, subsequent

lidocaine microinfusion into the same group of mice was able to attenuate taste preference (Supplementary Fig. 4e). Thus, in two behavioral paradigms Src40-49Tat did not affect learning and memory.

### Suppression of inflammatory pain behaviors requires Src

We investigated Src-dependency of effects of Src40-49Tat on inflammatory pain behaviors using *Src* null mutant mice<sup>32</sup>. *Src*<sup>-/-</sup> mice were not different from wild-type littermate controls in acute thermal or mechanical nociceptive responses, in locomotor function as measured by the accelerated rota-rod test (Supplementary Fig. 5a–d), in Morris water maze testing or in contextual fear conditioning (Supplementary Fig. 5 e,f). Formalin-induced behaviors in phase 1 were unaltered in *Src*<sup>-/-</sup> mice (Fig. 5a). However, formalin-induced behaviors in phase 2 were significantly reduced in *Src* null mutant mice as compared with wild-type littermate controls (Fig. 5a,b). There was no difference between wild-type and *Src*<sup>-/-</sup> mice in the basal level of tyrosine phosphorylation of NR2B in dorsal spinal cord (Supplementary Fig. 6a). However, after formalin administration, the increase in tyrosine phosphorylation of NR2B in the spinal dorsal horn in the wild-type did not occur in *Src*<sup>-/-</sup> mice (Fig. 5c). Thus, as anticipated from our findings with administering Src40-49Tat, formalin-induced behaviors in the second phase, but not in the first phase, and formalin-induced NR2B tyrosine phosphorylation in the dorsal horn are dependent upon Src.

We reasoned that if the effects of Src40-49Tat are mediated by uncoupling of Src from the NMDAR complex, then these effects will be lost in the absence of Src. To test this, we compared the effect of Src40-49Tat on formalin-induced behaviors in *Src*<sup>-/-</sup> versus wild-type littermates. As with our findings using rats, administering Src40-49Tat *i.v.* 45 min before formalin in wild-type mice had no effect on phase 1 behaviors (Fig. 5d) but significantly reduced formalin-induced phase 2 behaviors (Fig. 5d,e). By contrast, in the *Src* null mutant mice, intravenously administered Src40-49Tat had no effect on formalin-induced phase 2 behaviors (Fig. 5f; Supplementary Figure 6b,c). Because phase 2 behaviors were suppressed in *Src*<sup>-/-</sup> mice but were not further inhibited by Src40-49Tat, we infer that the effect of the peptide was occluded in the *Src* null mutant mice. Formalin-induced behaviors in *Src*<sup>-/-</sup> mice were suppressed by morphine (Supplementary Fig. 7a), indicating that these mice are not generally resistant to analgesics. Thus, our results indicate that the suppression of inflammatory pain behaviors by Src40-49Tat is Src-dependent.

### Src40-49Tat reverses nerve-induced pain behaviors

We next tested Src40-49Tat on neuropathic pain behaviors using a model of peripheral nerve injury (PNI) in rats characterized by a reduction of mechanical paw withdrawal threshold and cold-induced sensitization<sup>33,34</sup>. The effect of Src40-49Tat on mechanical withdrawal threshold was assessed 8–15 d after PNI<sup>5,35</sup>. We found that Src40-49Tat, but not sSrc40-49Tat or saline vehicle, caused a significant increase in paw withdrawal threshold ipsilateral to the nerve injury when administered either intrathecally (Fig. 6a) or intravenously (Fig. 6b). The increase in paw withdrawal threshold developed within the first hour, and with intrathecal administration the effect persisted for the 5-h testing period. With intravenous administration, the increase in paw withdrawal threshold peaked approximately 2 h after injecting Src40-49Tat. With either intrathecal or intravenous administration, paw

withdrawal threshold had returned to the pre-injection level by 24 h after the peptide was injected (data not illustrated).

Cold-induced sensitization was assessed by applying a drop of acetone to the plantar surface of the paw, which evokes flinching, and licking or biting behaviors<sup>36</sup>. Administering Src40-49Tat significantly reduced acetone-induced behaviors but sSrc40-49Tat had no effect (Fig. 6c; Supplementary Fig. 7b).

We found that the level of tyrosine phosphorylation of NR2B in the ipsilateral spinal cord was significantly increased by PNI with no effect on total NRB (Fig. 6d). Intrathecal administration of Src40-49Tat reduced the level of NR2B tyrosine phosphorylation in PNI animals to a level not different from that in sham controls (Fig. 6d). Collectively, our results indicate that Src40-49Tat reverses PNI-induced mechanical and cold sensitization and that, acting at the level of the spinal cord, Src40-49Tat normalizes PNI-induced NR2B tyrosine phosphorylation.

We tested Src-dependency of PNI-induced mechanical hypersensitivity by comparing *Src*<sup>-/-</sup> mice and wild-type littermate controls. In wild-type mice, PNI caused a marked reduction in paw withdrawal threshold of the ipsilateral paw beginning one day following PNI and persisting for more than 3 weeks (Fig. 6e). In *Src*<sup>-/-</sup> mice the reduction in paw withdrawal threshold was significantly less than that in the wild-type mice throughout the 22-d period during which the mice were examined (Fig. 6e). Correspondingly, the PNI-induced increase in tyrosine phosphorylation of NR2B in the ipsilateral dorsal spinal cord was reduced in *Src*<sup>-/-</sup> mice compared with that in wild-type littermates (Fig. 6e inset). Src40-49Tat *i.v.* significantly increased paw withdrawal threshold in wild-type mice 14 d after PNI, (Fig. 6f), to a level not different from that in the *Src*<sup>-/-</sup> mice without peptide administration (Fig. 6f). However, Src40-49Tat had no effect on paw withdrawal threshold in the *Src* null mutant mice. Likewise, when administered 3 d after PNI, Src40-49Tat significantly increased paw withdrawal threshold in wild-type mice but not in *Src*<sup>-/-</sup> mice (Supplementary Fig. 7c). Thus, we concluded that the suppression of mechanical hypersensitivity by Src40-49 was occluded in *Src*<sup>-/-</sup> mice, and as such, that this effect is Src-dependent.

## DISCUSSION

Our findings show that the Src40-49Tat peptide, but not the scrambled Src40-49Tat peptide, suppresses pain hypersensitivity induced by inflammation and peripheral nerve injury. By contrast, Src40-49Tat caused no alteration in acute thermal, mechanical or chemical nociception. Because there appeared to be no confounding sedative, motor depressant, or cognitive effects of the peptide (see Supplementary Discussion), we conclude that Src40-49Tat suppresses pain hypersensitivity, and that behaviors in models of chronic pain are suppressed preferentially with respect to those in acute nociception. Moreover, in *Src* null mutant mice both the formalin- and PNI-induced pain hypersensitivity were reduced and the effects of Src40-49Tat were occluded in these animals. Together these findings demonstrate that a common link between inflammatory and neuropathic pain behaviors is dependency upon Src. The most parsimonious interpretation of our findings is that the suppression of pain hypersensitivity behaviors by Src40-49Tat may be mediated by



disruption of the Src-ND2 interaction and subsequent inhibition of Src-induced enhancement of NMDAR function.

We designed Src40-49Tat to inhibit the interaction of Src with its anchoring protein, ND2, in the NMDAR complex. The binding of Src40-49Tat to ND2 in and of itself cannot account for the behavioral effects of the peptide, because the ND2 level within the NMDAR complex is not changed in *Src* null mice<sup>37</sup>, and yet the pain hypersensitivity was not affected by Src40-49Tat in these animals. By similar reasoning, potential binding of Src40-49Tat to molecules other than ND2 may remain in *Src*<sup>-/-</sup> mice and thus, such off-target interactions, if they exist, are not responsible for the suppression of pain hypersensitivity by the peptide. Rather, the suppression of pain hypersensitivity by Src40-49Tat may require an intact interaction between Src and ND2, which is inhibited by the peptide. It is conceivable that Src40-49Tat might inhibit an interaction of Src with a partner other than ND2, that has the same Src40-49 binding motif as does ND2. However, the Src-binding region of ND2, which is highly conserved in mouse, rat and humans<sup>18</sup>, contains no known conserved domains or motifs, and shows minimal primary sequence homology to other proteins.

Within the NMDAR complex, Src enhances NMDAR function by increasing channel open time and open probability upon binding of the co-agonists glutamate and glycine, leading to increased synaptic NMDARs currents<sup>14</sup>. Src is opposed by the phosphotyrosine phosphatase STEP<sup>21</sup>, and the balance of the activity between these two enzymes provides dynamic gain control of NMDAR function<sup>16</sup>. Our findings indicate that peripheral inflammation causes a rapid onset and sustained Src-dependent increase in tyrosine phosphorylation, which may enhance the function of NMDARs in the spinal cord. The reversal of the decreased paw withdrawal threshold by Src40-49Tat several weeks after PNI likewise implies that there is an ongoing increase in Src activity relative to STEP, which is required to sustain pain hypersensitivity after PNI. Many candidate intracellular signaling pathways might cause the relative increase in Src activity within the NMDAR complex<sup>16,38,39</sup> that produces pain hypersensitivity, and it is conceivable these pathways may be common, or distinct, for inflammatory versus neuropathic pain.

The kinase most closely related to Src is Fyn, and PNI-induced behaviors are suppressed in *Fyn* null mutant mice<sup>40</sup>, indicating that Fyn may also be important for these behaviors. It is known that Fyn does not interact with ND2<sup>18</sup> and here we found that Src40-49Tat does not affect the association of Fyn with NMDARs. Moreover, the effects of Src40-49Tat were prevented in *Src*<sup>-/-</sup> mice, which do express Fyn. Collectively, these findings indicate that Src40-49Tat does not act directly through Fyn. In the case of PNI, it is possible that Fyn may be downstream of Src and hence, that Fyn might be indirectly affected by Src40-49Tat.

Inhibitors of Src family kinases (SFKs) targeting the catalytic domain have been reported to reduce CFA-induced mechanical hyperalgesia<sup>41</sup> and PNI-induced behaviors<sup>42</sup>, and we show here that PP2 reduces CFA-induced thermal hyperalgesia. SFK inhibitors do not distinguish well between members of the Src family<sup>43</sup>. By contrast, Src40-49 corresponds to a sequence in the unique domain, which has no primary sequence homology to that in any other SFK. Catalytic domain inhibitors block the kinase regardless of substrate. However, Src40-49Tat does not inhibit kinase catalytic activity but rather separates the kinase from its substrate.

Thus, two strategic advantages of Src40-49Tat are that it suppresses the action of Src differentially from other SFKs, and that it does this only for substrates where Src targeting to the protein depends upon the Src-ND2 interaction, as does that of the NMDAR<sup>18</sup>.

Distinguishing between inflammatory versus neuropathic pain may be difficult clinically. Thus, an efficacious therapy that simultaneously suppresses both inflammatory and neuropathic pain, and at the same time has a wide therapeutic window, would have the advantage of being effective and safe, and could simplify pain management strategies. Our present discoveries open up the possibility that such a therapeutic approach may be achieved by targeting the Src-mediated enhancement of NMDAR function. NMDARs are implicated in many disease processes in the CNS, including neurodegenerative disorders, epilepsy and stroke. From our present findings it is possible that potentiated NMDAR function, by Src or other pathways, rather than basal receptor function, is crucial for these disorders as well. Thus, our findings reveal a strategy relevant to the treatment of chronic pain, and potentially other NMDAR-dependent CNS pathologies.

## METHODS

### Animals

All animals were used in accordance with the guidelines of the Canadian Council on Animal Care. Male Sprague–Dawley rats used for behavioral studies were purchased from Charles River, Montreal QC. The *c-Src* null mutation was introduced by homologous recombination into embryonic stem cells as described previously<sup>32</sup>. The mice used in contextual fear and CTA experiments were the offspring (F1) from a cross between C57Bl/6Tac (B6; Taconic Farms) and 129Sv/Tac (129; Taconic Farms). Mice were bred in the animal colony at the Hospital for Sick Children according to Research Institute guidelines. ANOVA or Student's *t* test were used to determine significant differences between sample groups for behavioral testing.  $p < 0.05$  was considered significant in all cases.

### Models for inflammatory or neuropathic pain

To produce inflammatory pain, formalin (2.5%, 50  $\mu$ l for rats, 1.5%, 20  $\mu$ l for mice) or Complete Freund's adjuvant (CFA) (0.05ml of *Mycobacterium tuberculosis*) was subcutaneously injected into the plantar hindpaw. For the formalin test, two animals in adjacent chambers were observed at one time, for flinching behaviors or biting and licking time<sup>44</sup> with observations occurring in alternate 2 min period out of a 4 min bin. Data were presented either as time course, or cumulative number of flinches and the total amount of time with biting and licking behaviors during phase 1 (0–8 min) or phase 2 (9–60 min). For the CFA model, thermal paw withdrawal latency (PWL)<sup>28, 45</sup> and mechanical paw withdrawal threshold (PWT) were measured. Data were presented either as a raw data or normalized for each animal as the percentage Maximal Possible Effect (MPE) in terms of the change in the PWL ipsilateral to CFA. These values were calculated as follows: Percentage MPE =  $(\text{Time}_X \text{ PWL} - \text{Time}_0 \text{ PWL}) / (\text{baseline} - \text{Time}_0 \text{ PWL})$ . Time<sub>0</sub> is the PWL 24 h following CFA, before drug administration. Time<sub>X</sub> is the time point following Src40-49Tat, PP2 or their respective controls injection. To produce peripheral nerve injury (PNI), a polyethylene cuff (2 mm in length) was surgically implanted around the sciatic



nerve of rats or mice under isoflurane anesthesia<sup>5,35</sup> Mechanical paw withdrawal threshold<sup>5, 35</sup> and cold sensitization<sup>36</sup> were measured as previously described. See Supplementary Methods online for details of thermal paw withdrawal latency testing, mechanical paw withdrawal threshold testing, and cold sensitization testing.

## Peptides

Src40-49 (KPASADGHRG), scrambled Src40-49 (GAAKRPSDGH), Tat protein transduction domain (YGRKKRRQRRR), Src40-49Tat (KPASADGHRGYGRKKRRQRRR) and scrambled Src40-49Tat (GAAKRPSDGHYGRKKRRQRRR) were synthesized by the Advanced Protein Technology Center, Toronto, Canada.

## Co-Immunoprecipitation, Immunoprecipitation and Immunoblotting

For co-immunoprecipitation NMDAR and its associated proteins, crude synaptosomal fraction from forebrain or spinal cord was prepared as described previously<sup>21</sup>. For *in vitro* competition experiments, Src40-49Tat or Scrambled Src40-49Tat, (10 $\mu$ M), was incubated with the lysate 30 min before adding antibody for immunoprecipitation.

For immunoprecipitation to examine the relative tyrosine phosphorylation of NR2B, we rapidly removed the dorsal lumbar spinal cord ipsilateral to formalin or CFA or PNI. Each sample contained proteins from one animal, and was homogenized, immunoprecipitated and analyzed individually. Spinal cord was homogenized as described<sup>41</sup> in ice cold RIPA buffer. centrifuged and the protein concentration determined. Samples were then incubated with NR2B antiserum (Santa Cruz Biotechnology) overnight. Immune complexes were isolated by protein G-Sepharose beads, resolved by SDS-PAGE and transferred to nitrocellulose membranes. Membranes were first probed with an antibody against phosphotyrosine, then stripped and reprobred with an antibody against NR2B. For densitometric quantification, immunoblots were digitized and quantified using ImageJ software. The relative phosphotyrosine NR2B band density (relative p-NR2B density) levels were obtained by normalizing the anti-phosphotyrosine immunoblot against the corresponding NR2B subunit immunoblot from the same sample. A linear detection range was established for each antibody used, and only values falling in this linear range were incorporated into the final quantitative analysis. ANOVA and an unpaired two-tailed *t* test were used to determine significant differences between sample groups. *p* < 0.05 was considered significant in all cases.

## Electrophysiological recordings

Whole-cell recordings were made from cultured dorsal horn neurons as described<sup>20</sup>. Src(40-49) or sSrc(40-49) were added to the intracellular solution for a final concentration of 0.015 mg ml<sup>-1</sup>. Whole-cell currents were recorded with an AxoPatch 200B amplifier (Axon Instruments), digitized (20 KHz) and analyzed offline. Detection and analysis of mEPSCs was done off-line (MiniAnalysis Program, Synaptosoft). Average mEPSCs observed in the first two min after breaking in whole-cell configuration were used as control and compared to averages obtained after 8–14 min in whole-cell. The AMPA component was measured at the maximum amplitude during the first 5 ms in each event and the NMDA

component as the integrated charge between 5–150 ms after the peak value<sup>15</sup>. Mean mEPSCs contained at least 30 traces. See Supplementary Methods online for more details.

## Supplementary Material

Refer to Web version on PubMed Central for supplementary material.

## Acknowledgments

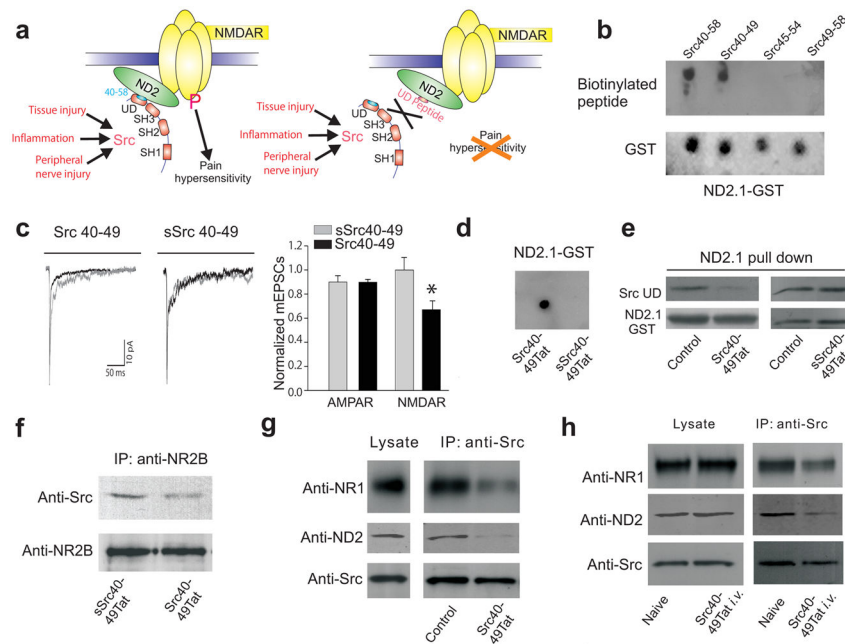
Supported by grants from the Canadian Institutes of Health Research (CIHR; grant number MT-12682) and the Neuroscience Canada Brain Repair Program to MWS. MWS is an International Research Scholar of the Howard Hughes Medical Institute and holds a Canada Research Chair (Tier I) in Neuroplasticity and Pain. XJL is a CIHR & Ronald Melzack Pain Research Award recipient, and a fellow of Canadian Arthritis Network as well as of the Pain: Molecules to Community Strategic Training Initiative in Health Research of CIHR. MVC is an International Fellow of the Wellcome Trust UK. Src knockout mice were obtained as gift from B.F. Boyce, University of Rochester Medical Center, Rochester, USA. We thank S. Singhroy and D. Wong for technical support, T. Trang, and J. Hicks for helpful comments on the manuscript.

## Reference List

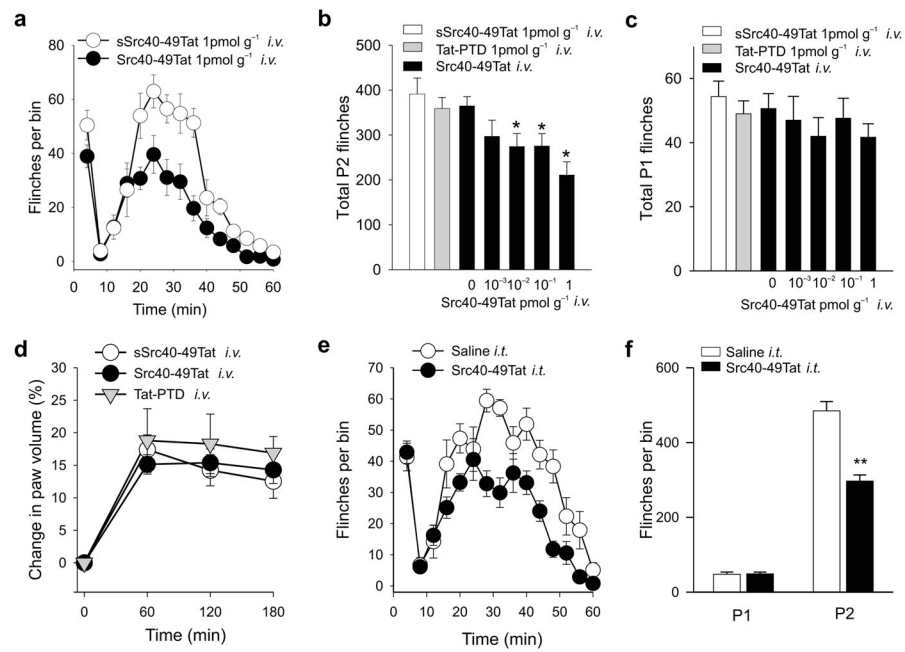
1. Woolf CJ, Salter MW. Neuronal plasticity: increasing the gain in pain. *Science*. 2000; 288:1765–1769. [PubMed: 10846153]
2. Ji RR, Strichartz G. Cell signaling and the genesis of neuropathic pain. *Sci STKE*. 2004; 2004:reE14. [PubMed: 15454629]
3. Julius D, Basbaum AI. Molecular mechanisms of nociception. *Nature*. 2001; 413:203–210. [PubMed: 11557989]
4. Woolf CJ, Costigan M. Transcriptional and posttranslational plasticity and the generation of inflammatory pain. *Proc Natl Acad Sci U S A*. 1999; 96:7723–7730. [PubMed: 10393888]
5. Coull JA, et al. BDNF from microglia causes the shift in neuronal anion gradient underlying neuropathic pain. *Nature*. 2005; 438:1017–1021. [PubMed: 16355225]
6. Marchand F, Perretti M, McMahon SB. Role of the immune system in chronic pain. *Nat Rev Neurosci*. 2005; 6:521–532. [PubMed: 15995723]
7. Scholz J, et al. Blocking caspase activity prevents transsynaptic neuronal apoptosis and the loss of inhibition in lamina II of the dorsal horn after peripheral nerve injury. *J Neurosci*. 2005; 25:7317–7323. [PubMed: 16093381]
8. Dingledine R, Borges K, Bowie D, Traynelis SF. The glutamate receptor ion channels. *Pharmacol Rev*. 1999; 51:7–61. [PubMed: 10049997]
9. Bleakman D, Alt A, Nisenbaum ES. Glutamate receptors and pain. *Semin Cell Dev Biol*. 2006; 17:592–604. [PubMed: 17110139]
10. Brown DG, Krupp JJ. N-Methyl-D-Aspartate Receptor (NMDA) Antagonists as Potential Pain Therapeutics. *Curr Top Med Chem*. 2006; 6:749–770. [PubMed: 16719815]
11. Petrenko AB, Yamakura T, Baba H, Shimoji K. The role of N-methyl-D-aspartate (NMDA) receptors in pain: a review. *Anesth Analg*. 2003; 97:1108–1116. [PubMed: 14500166]
12. Muir KW. Glutamate-based therapeutic approaches: clinical trials with NMDA antagonists. *Curr Opin Pharmacol*. 2006; 6:53–60. [PubMed: 16359918]
13. Smith PF. Therapeutic N-methyl-D-aspartate receptor antagonists: will reality meet expectation? *Curr Opin Investig Drugs*. 2003; 4:826–832.
14. Yu XM, Salter MW. Src, a molecular switch governing gain control of synaptic transmission mediated by N-methyl-D-aspartate receptors. *Proc Natl Acad Sci U S A*. 1999; 96:7697–7704. [PubMed: 10393883]
15. Yu XM, Askalan R, Keil GJ, Salter MW. NMDA channel regulation by channel-associated protein tyrosine kinase Src. *Science*. 1997; 275:674–678. [PubMed: 9005855]
16. Salter MW, Kalia LV. Src kinases: a hub for NMDA receptor regulation. *Nat Rev Neurosci*. 2004; 5:317–328. [PubMed: 15034556]

17. Furukawa H, Singh SK, Mancusso R, Gouaux E. Subunit arrangement and function in NMDA receptors. *Nature*. 2005; 438:185–192. [PubMed: 16281028]
18. Gingrich JR, et al. Unique domain anchoring of Src to synaptic NMDA receptors via the mitochondrial protein NADH dehydrogenase subunit 2. *Proc Natl Acad Sci U S A*. 2004; 101:6237–6242. [PubMed: 15069201]
19. Erpel T, Courtneidge SA. Src family protein tyrosine kinases and cellular signal transduction pathways. *Curr Opin Cell Biol*. 1995; 7:176–182. [PubMed: 7612268]
20. Salter MW, Hicks JL. ATP-evoked increases in intracellular calcium in neurons and glia from the dorsal spinal cord. *J Neurosci*. 1994; 14:1563–1575. [PubMed: 8126555]
21. Pelkey KA, et al. Tyrosine phosphatase STEP is a tonic brake on induction of long-term potentiation. *Neuron*. 2002; 34:127–138. [PubMed: 11931747]
22. Huang Y, et al. CAKbeta/Pyk2 kinase is a signaling link for induction of long-term potentiation in CA1 hippocampus. *Neuron*. 2001; 29:485–496. [PubMed: 11239437]
23. Schwarze SR, Ho A, Vocero-Akbani A, Dowdy SF. In vivo protein transduction: delivery of a biologically active protein into the mouse. *Science*. 1999; 285:1569–1572. [PubMed: 10477521]
24. Dubuisson D, Dennis SG. The formalin test: a quantitative study of the analgesic effects of morphine, meperidine, and brain stem stimulation in rats and cats. *Pain*. 1977; 4:161–174. [PubMed: 564014]
25. Wheeler-Aceto H, Cowan A. Standardization of the rat paw formalin test for the evaluation of analgesics. *Psychopharmacology (Berl)*. 1991; 104:35–44. [PubMed: 1882002]
26. Sawynok J, Liu XJ. Formalin test: Characteristics and the usefulness of the model. *Reviews Analgesia*. 2004; 7:145–163.
27. Wheeler-Aceto H, Porreca F, Cowan A. The rat paw formalin test: comparison of noxious agents. *Pain*. 1990; 40:229–238. [PubMed: 2308768]
28. Hargreaves K, Dubner R, Brown F, Flores C, Joris J. A new and sensitive method for measuring thermal nociception in cutaneous hyperalgesia. *Pain*. 1988; 32:77–88. [PubMed: 3340425]
29. Bast T, Zhang WN, Feldon J. Dorsal hippocampus and classical fear conditioning to tone and context in rats: effects of local NMDA-receptor blockade and stimulation. *Hippocampus*. 2003; 13:657–675. [PubMed: 12962312]
30. Rosenblum K, et al. Modulation of protein tyrosine phosphorylation in rat insular cortex after conditioned taste aversion training. *Proc Natl Acad Sci U S A*. 1995; 92:1157–1161. [PubMed: 7862652]
31. Berman DE, Dudai Y. Memory extinction, learning anew, and learning the new: dissociations in the molecular machinery of learning in cortex. *Science*. 2001; 291:2417–2419. [PubMed: 11264539]
32. Soriano P, Montgomery C, Geske R, Bradley A. Targeted disruption of the c-src proto-oncogene leads to osteopetrosis in mice. *Cell*. 1991; 64:693–702. [PubMed: 1997203]
33. Woolf CJ, Mannion RJ. Neuropathic pain: aetiology, symptoms, mechanisms, and management. *Lancet*. 1999; 353:1959–1964. [PubMed: 10371588]
34. Dworkin RH, et al. Advances in neuropathic pain: diagnosis, mechanisms, and treatment recommendations. *Arch Neurol*. 2003; 60:1524–1534. [PubMed: 14623723]
35. Pitcher GM, Ritchie J, Henry JL. Paw withdrawal threshold in the von Frey hair test is influenced by the surface on which the rat stands. *J Neurosci Methods*. 1999; 87:185–193. [PubMed: 11230815]
36. Saade NE, et al. Spinal pathways involved in supraspinal modulation of neuropathic manifestations in rats. *Pain*. 2006; 126:280–293. [PubMed: 16945485]
37. Gingrich, JR. Thesis. 2004. Unique domain anchoring of Src to synaptic NMDA receptors via the mitochondrial protein NADH dehydrogenase subunit 2.
38. Xu J, et al. Control of excitatory synaptic transmission by C-terminal SRC kinase. *J Biol Chem*. 2008
39. Kalia LV, Pitcher GM, Pelkey KA, Salter MW. PSD-95 is a negative regulator of the tyrosine kinase Src in the NMDA receptor complex. *EMBO J*. 2006; 25:4971–4982. [PubMed: 16990796]

40. Abe T, et al. Fyn kinase-mediated phosphorylation of NMDA receptor NR2B subunit at Tyr1472 is essential for maintenance of neuropathic pain. *Eur J Neurosci.* 2005; 22:1445–1454. [PubMed: 16190898]
41. Guo W, et al. Tyrosine phosphorylation of the NR2B subunit of the NMDA receptor in the spinal cord during the development and maintenance of inflammatory hyperalgesia. *J Neurosci.* 2002; 22:6208–6217. [PubMed: 12122079]
42. Katsura H, et al. Activation of Src-family kinases in spinal microglia contributes to mechanical hypersensitivity after nerve injury. *J Neurosci.* 2006; 26:8680–8690. [PubMed: 16928856]
43. Chong YP, Ia KK, Mulhern TD, Cheng HC. Endogenous and synthetic inhibitors of the Src-family protein tyrosine kinases. *Biochim Biophys Acta.* 2005; 1754:210–220. [PubMed: 16198159]
44. Liu XJ, White TD, Sawynok J. Potentiation of formalin-evoked adenosine release by an adenosine kinase inhibitor and an adenosine deaminase inhibitor in the rat hind paw: a microdialysis study. *Eur J Pharmacol.* 2000; 408:143–152. [PubMed: 11080520]
45. Liu XJ, Sawynok J. Peripheral antihyperalgesic effects by adenosine A<sub>1</sub> receptor agonists and inhibitors of adenosine metabolism in a rat neuropathic pain model. *Analgesia.* 2001; 5:19–29.

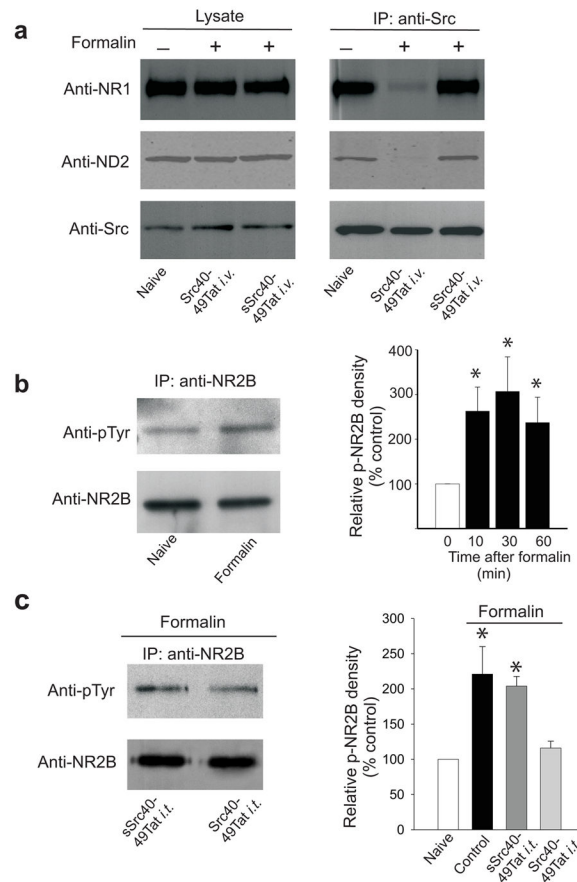


**Fig. 1.** Src40-49Tat suppresses the Src-NMDAR interaction *in vitro* and *in vivo*. **(a)** Cartoon illustrating the main hypothesis. Domain structure of Src shows Src-homology (SH) domains 1,2,3 and the unique domain (UD). **(b)** Dot blot of ND2.1-GST fusion protein probed with biotinylated Src unique domain peptide with overlapping sequence of 40-58, followed by streptavidin-HRP (SA-HRP). **(c)** Effect of Src 40-49 on mEPSCs. Left panel, average mEPSCs in the first two min after breaking in to whole-cell configuration was superimposed with averages obtained after 8–14 min. Right panel: the ratio of measurements during the first two min and from 8–14 min (Src40-49 n = 11; sSrc40-49 n = 5). **(d)** Dot blot of ND2.1-GST fusion protein probed with biotinylated Src40-49Tat or scrambled Src40-49Tat followed by SA-HRP. **(e)** *In vitro* binding assay of assays with ND2.1-GST and Src unique domain, with no peptide, Src40-49Tat or sSrc40-49Tat (30 μM). Src unique domain bound to ND2.1-GST was probed with antibody against Src, stripped and reprobed with antibody against GST. **(f–h)** Immunoblots of coimmunoprecipitates obtained with antibody against NR2B (anti-NR2B, **f**) or antibody against Src (anti-Src, **g–h**) from brain crude synaptosomes (**f–g**) *in vitro* incubated with Src40-49Tat or sSrc40-49Tat (10 μM) or **(h)** from animals with or without Src40-49Tat (100 pmol g<sup>-1</sup>) intravenous injection (45 min before sample collection). Blots were probed with respective antibodies as labeled.

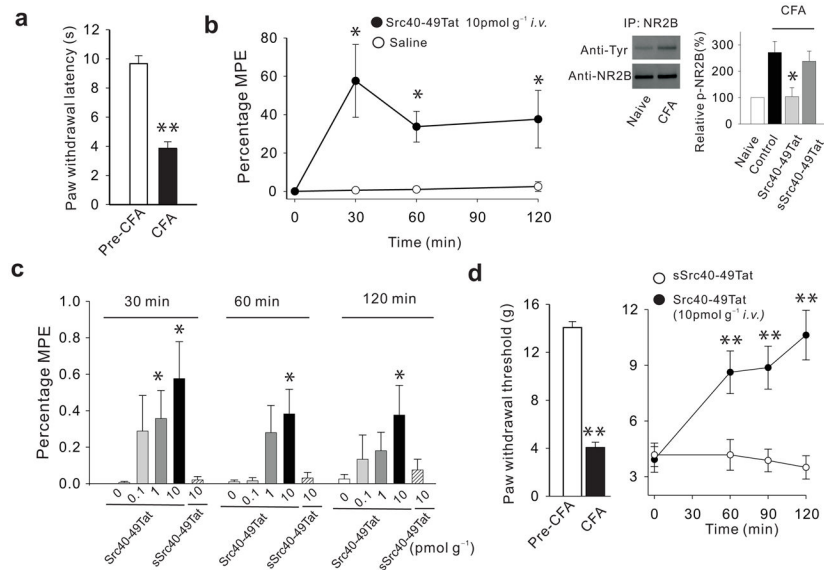


**Fig. 2.** Src40-49Tat suppresses formalin-induced behaviors in rats with intravenous or intrathecal administration. **(a)** Time course of flinches induced by formalin (2.5%), with Src40-49Tat ( $1\text{ pmol g}^{-1}$ , *i.v.*) or sSrc40-49Tat ( $1\text{ pmol g}^{-1}$ , *i.v.*) 45 min before formalin ( $n=10$ ). **(b–c)** The effect of Src40-49Tat ( $0.001\text{--}10\text{ pmol g}^{-1}$ , *i.v.*,  $n=10$ ) on formalin-induced phase 2 (9–60 min, **b**) or phase 1 (0–8 min, **c**) flinches. Scrambled Src40-49Tat ( $1\text{ pmol g}^{-1}$ ,  $n=10$ ), Tat-protein transduction domain alone (Tat-PTD) ( $1\text{ pmol g}^{-1}$ ,  $n=10$ ) or saline vehicle ( $n=28$ ) were used as controls (\* $p<0.05$  vs. saline controls). **(d)** The effect of Src40-49Tat, Scrambled Src40-49Tat or Tat-PTD (*i.v.*,  $1\text{ pmol g}^{-1}$ ,  $n=8$ ) on formalin-induced paw edema. **(e–f)** The effect of intrathecal Src40-49Tat ( $5\times 10^{-4}\text{ pmol g}^{-1}$ , 30 min pretreatment) on formalin-induced flinches. **(e)** time course, **(f)** total number of flinches ( $n=8$ , \*\* $p<0.01$  vs. saline treated controls). (mean $\pm$ s.e.m. for all groups)

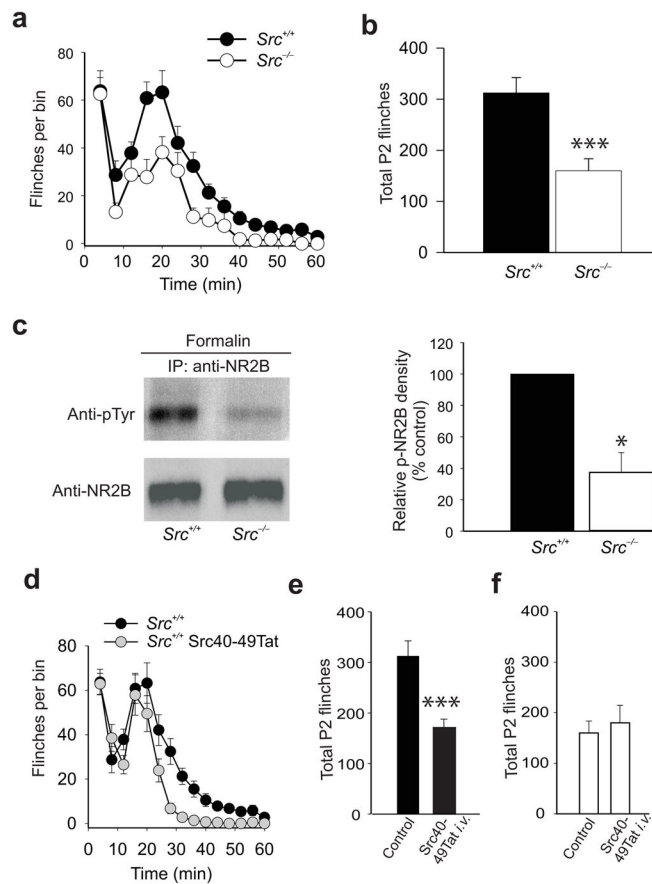




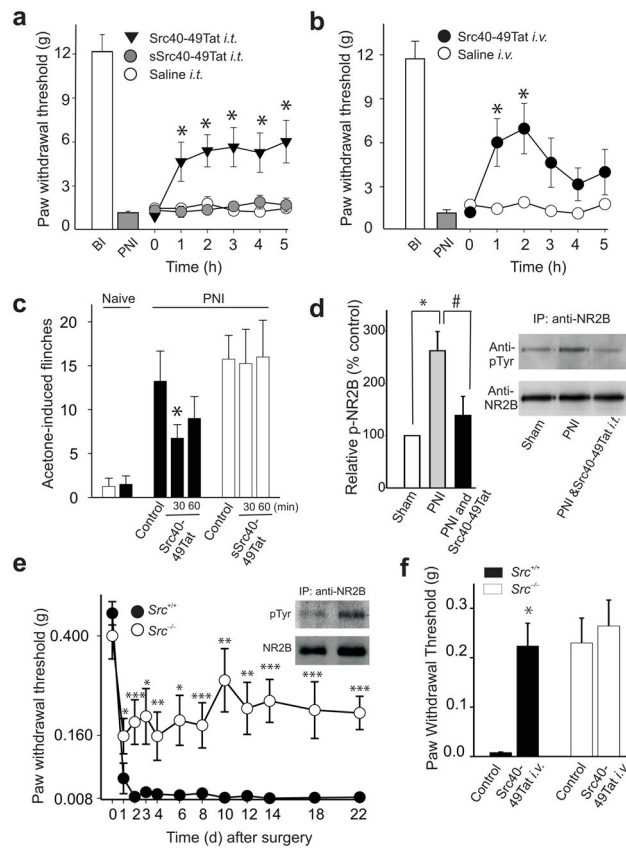
**Fig. 3.** Src40-49Tat disrupts Src association with ND2 and with NMDAR, and prevents formalin-induced increase in tyrosine phosphorylation of the NR2B in spinal cord dorsal horn. **(a)** Representative immunoblots of lysate (left) or co-immunoprecipitates obtained with antibody against Src from spinal cord crude synaptosomes in naïve animals, or in animals with Src40-49Tat and sSrc40-49Tat ( $10\text{ pmol g}^{-1}$ , *i.v.*, 45 before formalin). Samples were collected 30 min following formalin. The blots were probed with antibody against NR1, and stripped and re-probed with antibodies against ND2 and against Src. **(b-c)** Representative immunoblots (left panel) of immunoprecipitates obtained with antibody against NR2B from ipsilateral dorsal lumbar spinal cord following formalin injection, probed with antibodies against phosphotyrosine (anti-pTyr) and against NR2B. Right panel shows a histogram of relative tyrosine phosphorylation of NR2B (Relative p-NR2B density; see Methods), normalized to naïve. **(b)** Samples were collected in naïve rats or at 10, 30, and 60 min following formalin injection, **(c)** Rats were treated intrathecally with Src40-49Tat or sSrc40-49Tat ( $5 \times 10^{-4} \text{ pmol g}^{-1}$ ), and samples were collected 60 min following formalin injection. (mean  $\pm$  s.e.m.;  $n=6-10$ , each analyzed individually \* $p < 0.05$  vs. naïve control).



**Fig. 4.** Src40-49Tat reverses CFA-induced thermal and mechanical hypersensitivity. **(a)** CFA injection reduces ipsilateral paw withdrawal latency (PWL) to radiant heat 24 h following CFA. **(b)** The effect of Src40-49Tat (10 pmol g<sup>-1</sup>, *i.v.*) on CFA-induced thermal hypersensitivity in terms of percentage Maximal Possible Effect (MPE; see Methods) of PWL. Inset: immunoblot and histogram showing tyrosine phosphorylation of NR2B 24 h after CFA and effects of Src40-49Tat or sSrc40-49Tat on normalized p-NR2B band intensity. **(c)** Histogram illustrating effects Src40-49Tat (0.1, 1 or 10 pmol g<sup>-1</sup>, *i.v.*) or of sSrc40-49Tat (10 pmol g<sup>-1</sup>, *i.v.*) or saline (0) on CFA-induced changes in PWL, expressed as percentage MPE of PWL. **(d)** The effect of Src40-49Tat and sSrc40-49Tat (10pmol g<sup>-1</sup> *i.v.*) on CFA-induced reduction of paw withdrawal threshold (PWT) to Von-Frey stimuli in the ipsilateral paw, 6 h following CFA. (\**p*<0.05, \*\**p*<0.01 vs. control; mean±s.e.m.; n=5–9).



**Fig. 5.** The effect of Src40-49Tat on formalin-induced behavior is occluded in *Src* null mutant mice. Time course (**a**) and total phase 2 flinches (**b**) induced by 1.5% formalin in *Src*<sup>-/-</sup> mice and littermate wild-type mice (mean±s.e.m, n=5 mice, \*\*\*p<0.005 vs. wild-type littermate control, *Src*<sup>+/+</sup>). (**c**) Representative immunoblots (left panel) of immunoprecipitates obtained with NR2B antibody from spinal cord of *Src*<sup>-/-</sup> or *Src*<sup>+/+</sup> mice, 60 min after formalin injection. The immunoprecipitates were probed with antibodies against phosphotyrosine and against NR2B. Right panel: a histogram of relative p-NR2B band density of spinal dorsal horn from *Src*<sup>+/+</sup> and *Src*<sup>-/-</sup> mice treated with formalin, normalized to *Src*<sup>+/+</sup> mice (mean ±s.e.m.; n=3–7 mice, \*p<0.05 vs. wild-type littermates). (**d–f**) The effect of Src40-49Tat (0.5pmol g<sup>-1</sup> *i.v.*) on formalin-induced flinches in (**d–e**) wild-type control mice and (**f**) *Src* null mutant mice (mean±s.e.m., n=6–8 mice, \*\*\*p<0.005 vs. non-treated control mice).

**Fig. 6.**

The effect of Src40-49Tat on peripheral nerve injury-induced tactile and cold hypersensitivity. **(a–b)** The effect of Src40-49Tat on PNI-induced decrease of paw withdrawal thresholds (PWT) in rats with **(a)** intrathecal Src40-49Tat, sSrc40-49Tat ( $5 \times 10^{-4}$  pmol  $g^{-1}$ ) or **(b)** intravenous Src40-49Tat ( $10 \text{ pmol } g^{-1}$ ) administration. BI, before injury, PNI, peripheral nerve injury ( $n=10-16$ ,  $*p<0.05$ , vs. saline control). **(c)** The effect of Src40-49Tat on acetone-induced flinches in rats following PNI. Acetone was applied before or 30 and 60 min after Src40-49Tat or sSrc40-49Tat ( $10 \text{ pmol } g^{-1}$  *i.v.*) ( $*p<0.05$  vs. pre-peptide control,  $n=4$ ). **(d)** The effect of intrathecal Src40-49Tat ( $5 \times 10^{-4}$  pmol  $g^{-1}$ ) on PNI-induced increase in relative p-Tyr-NR2B density in rat spinal cord. Left panel: a histogram of the relative p-NR2B density normalized to sham, and right panel: representative immunoblots of immunoprecipitates obtained with antibody against NR2B and probed with antibodies against phosphotyrosine and against NR2B. (sample were collected 5 h following Src40-49Tat;  $n=5$ ,  $*p<0.05$  vs. sham;  $\#p<0.05$  vs. PNI). **(e)** PWT in *Src*<sup>-/-</sup> and *Src*<sup>+/+</sup> mice, day 1–22 after PNI. Inset: representative immunoblots of immunoprecipitates obtained with antibody against NR2B from spinal cord of *Src*<sup>-/-</sup> and *Src*<sup>+/+</sup> mice, 22 days following PNI, probed with antibodies against phosphotyrosine and against NR2B **(f)** The effect of Src40-49Tat ( $5 \text{ pmol } g^{-1}$ , *i.v.*) on PWT of *Src*<sup>-/-</sup> and *Src*<sup>+/+</sup> mice, day 14 after PNI **(e–f)**:  $n=8-11$ ,  $*p<0.05$ ,  $**p<0.01$ ,  $***p<0.001$  vs. controls). (mean $\pm$ s.e.m for all groups).